Journal of Applied Polymer Science

Melt processed elemental sulfur reinforced polyethylene composites

Kishore K. Jena, Saeed M. Alhassan
Department of Chemical Engineering, the Petroleum Institute, Abu Dhabi, United Arab Emirates
Correspondence to: S.M. Alhassan (E-mail: salhassan@pi.ac.ae)

ABSTRACT: Elemental sulfur represents a largely unutilized resource for high performance materials development. In this context, elemental sulfur was investigated as reinforcing agent for high density polyethylene (HDPE) composites via extrusion. We were able to produce homogenous composites with sulfur content up to 30 wt %. Compounding was done at 190°C well above the polymerization temperature of elemental sulfur. Infrared and Raman spectroscopy showed that sulfur did not undergo chemical reaction with HDPE. Additionally, Raman spectroscopy showed that sulfur exists in its most stable allotrope, cyclooctasulfur (S_8). Differential scanning calorimetry (DSC) showed that sulfur is present in non-orthorhombic crystal and X-ray diffraction confirms the same. Results suggest that sulfur is predominantly in its cyclooctasulfur allotrope and occupies the amorphous region of HDPE. According to TEM and SEM microscopy, the composites were of high quality, smooth and without distinguishable defects. Quality and smoothness of composites depend on the experimental parameters and sulfur loading. The addition of elemental sulfur significantly improved the elongation at break of the composites from 835 to 1202% (43% increases with 15 wt % sulfur) despite the obvious fact that HDPE possess an already impressive elongation at break quality. Such phenomena have not been reported in the literature. The improved composites would be suitable for a variety of engineering applications. © 2015 Wiley Periodicals, Inc. J. Appl. Polym. Sci. **2016**, *133*, 43060.

KEYWORDS: composites; differential scanning calorimetry; extrusion; mechanical properties

Received 20 March 2015; accepted 16 October 2015
DOI: 10.1002/app.43060

INTRODUCTION

Developing novel composite materials from elemental sulfur offers an exciting new direction in chemistry,[1,2] materials science[3] and chemical engineering.[4] Sulfur is the major by-product of hydrodesulfurization and sour gas processing intended to reduce sulfur dioxide emissions.[5] When elemental sulfur is heated it undergoes several transitions. Under ambient conditions elemental sulfur exists in the form of an eight-membered ring (S_8) orthorhombic crystal that undergoes solid-to-solid transition from orthorhombic crystal to monoclinic crystal (beta sulfur) at ~95°C. With further heating sulfur melts into a clear yellow liquid phase at 120–124°C. This is solid–liquid transition occurred in elemental sulfur. Rings with 8–35 sulfur atoms are formed and upon further heating of the liquid sulfur phase at 159°C and above results in equilibrium ring-opening polymerization (ROP) of the S_8 monomer into a linear polysulfane with diradical chain ends, which subsequently polymerizes into polymeric sulfur of high molecular weight.[4] It is widely known that this polymeric form of sulfur is not stable and reverts back to S_8 at room temperature and pressure.

Elemental sulfur is widely utilized for the production of sulfuric acid for fertilizers, synthetic rubber (via vulcanization processes) and cosmetics.[6–8] However, huge surplus of sulfur is generated annually due to lack of new demands for sulfur beyond the above classical applications.[4] A similar situation existed in 1970s because of newly imposed environmental regulations on emission of acid rain chemicals. That led to a short-lived renaissance in research on sulfur utilization.[9] Among the most promising applications are sodium sulfur battery and lithium sulfur battery. The recent advance in the field of lithium-sulfur batteries might lead to increase in the demand for sulfur.[10] Sulfur utilization by using "inverse vulcanization" process has been recently reported[1] where sulfur is copolymerized with dienes monomers to make random copolymers with sulfur content up to 90%. The copolymer was used as electroactive material in cathodes for Li–S batteries and for optical applications.[11] Contrariwise, elemental sulfur offers plethora of opportunities to explore several applications that do not require probing sulfur chemistry with other elements. Elemental sulfur by itself forms several allotropes, rings and polymers.[12,13] Additionally, elemental sulfur in its orthorhombic crystal structure has a band gap of 2.79 eV, which makes it a suitable material as photocatalyst.[14]

These interesting characteristics of the element offer opportunities beyond what has been reported in the literature.

With the extensive history of sulfur in polymer systems (rubber and copolymers), it has not been used as physical reinforcing agent in composite formulations with thermoplastics. Majority of research has been dedicated toward sulfur chemistry with polymers mainly because it forms radicals at moderate conditions. But the element has good mechanical and physical properties that make it suitable as passive filler in thermoplastics. Our proposed methodology offers the possibility of controlling the formation of several sulfur allotropes if processing conditions are designed properly. Such allotropes are deemed difficult to stabilize. Among these allotropes is the elusive polymeric sulfur,[15] which undergoes depolymerization at room temperature and pressure.[16,17] To this end, we focus our work on using elemental sulfur as filler for reinforcement of thermoplastic and producing different sulfur allotropes or/and forms that can enhance properties of host matrix. High density polyethylene (HDPE) was used as host matrix because it is widely used thermoplastic for many engineering applications and it is chemically inert. Additionally, our aim is to use elemental sulfur as reinforcing agent without inducing classical vulcanization or sulfurization reactions.[18] We have characterized the composites to understand the chemistry of sulfur in the host matrix as well as the thermal and mechanical properties of the composites. Here, we study the tensile mechanical behavior of the sulfur composites. This suggests that the sulfur composites can lead to dramatically enhanced Young's modulus as well as outstanding percentage of elongation under tensile loadings. To the best of our knowledge, this is the first comprehensive report on the use of elemental sulfur as a filler material and potentially modifying sulfur properties as way to reinforce host matrix.[19] In this work, we report on processing method for elemental sulfur as novel filler for composite materials with focus on spectroscopic and thermal characterization. Beside carbon, this work offers for the first time the ability to use an element, with allotropy as rich as carbon; in composite formulation.

EXPERIMENTAL SECTION AND MATERIALS

Materials

High-density polyethylene (HDPE) was obtained from BOROUGE, Abu Dhabi, United Arab Emirates. Before composite preparation, polyethylene pellets were dried at 70°C for 7 h in air circulated oven. TGA curve shows the purity of HDPE. Granulated elemental sulfur was supplied by Abu Dhabi Gas Industries Limited (GASCO, Abu Dhabi, United Arab Emirates) and used as received without further purification.

Synthesis of Sulfur Based Hybrid Composites

The elemental sulfur was incorporated into HDPE at 5–30 wt % loading. The components were melt-processed using a twin-screw Haake Minilab II compounder with screw diameter 5/14 mm conical and screw length 109.5mm. The barrel temperature was adjusted to 190°C heating with an average rotation of 100 rpm for all formulations. Composites were prepared by feeding HDPE first to the extruder followed by addition of the corresponding amount of sulfur (when sulfur and HDPE are compounded there are possibilities of formation of hydrogen sulfide (H_2S) or/and sulfur dioxide (SO_2); Extrusion must be done under inert conditions and with detectors for the above two toxic gases). Each composite was extruded under melt mixing for 15 min before injection molding. Pure HDPE was also passed through compounder under the same conditions to serve as a reference. After extruding, the material was cooled down to room temperature. The HDPE-S composites with different elemental sulfur content (5–30 wt %) were termed as HDPE-S-X (X= sulfur content) composites.

Analytical Techniques

Infrared spectra of the HDPE and HDPE-S composites were recorded by Attenuated total reflection Attenuated Totally Reflectance Fourier Transformed Infrared spectroscopy technique, using a Bruker Vertex 70. Each spectrum represents 60 scans rationed against a reference spectrum obtained by recording 60 scans of an empty ATR cell. Raman spectra were recorded on a Jobin Yvon Horiba LabRAM spectrometer with back-scattered confocal configuration using a HeNe laser (633 nm). A long working distance objective with magnification 50× was used both to collect the scattered light and to focus the laser beam on the sample surface. CCD (charge–coupled device) detector exposure time was 5 s and an average of 1cycle was used to increase S/N ratio. Diffraction (XRD) patterns were collected using analytical X'Pert PRO Powder Diffractometer (Cu-Kα radiation 1.5406 A°, 40 kV, 40 mA) in the range of 5°–80° 2θ scale, with a step size of 0.02°. The surface morphology of composites was characterized by scanning electron microscope (SEM, Quanta- FEG-250) and transmission electron microscope. Transmission electron microscopy (TEM) images were obtained using FEI Tecnai G20 operated at 200 kV accelerating voltage to observe the nanoscale structures of the sulfur in the composite. Samples were ultra-microtomed in room temperature conditions to prepare less than 100 nm thick samples. Differential Scanning Calorimetry (DSC) analysis of the composite samples (5–10 mg) was done using DSC Netzsch (Germany) at a heating rate of 10°C/min in the temperature range between −20 and 200°C in a nitrogen environment. The thermal degradation behavior was studied in TGA Netzsch Sta. 409 PC/PG (Germany). The samples (10-15 mg) were scanned from 25 to 900°C at a heating rate of 10°C/min in nitrogen environment. Tensile testing was carried out using an Instron 2519-107 universal testing machine (Instron Corp.), according to the ASTM standard test method D638−V. Testing was done at room temperature using plain rubber grips and the average of three replicas is reported here.

RESULTS AND DISCUSSION

Sample Preparation

Elemental sulfur exhibits rich allotropy.[12] This is evident by the long list of reported allotropes including S_2, S_3, S_4. . .S_x, where x can be up to 10^6! The most stable allotrope of sulfur is eight-membered ring, known as cyclooctasulfur or S_8 for short. This allotrope forms orthorhombic (alpha sulfur) crystals at room temperature and pressure. When elemental sulfur is heated it undergoes several transitions. First, it undergoes solid-to-solid transition from orthorhombic crystal to monoclinic crystal (beta sulfur) at ~95°C. With further heating sulfur undergoes

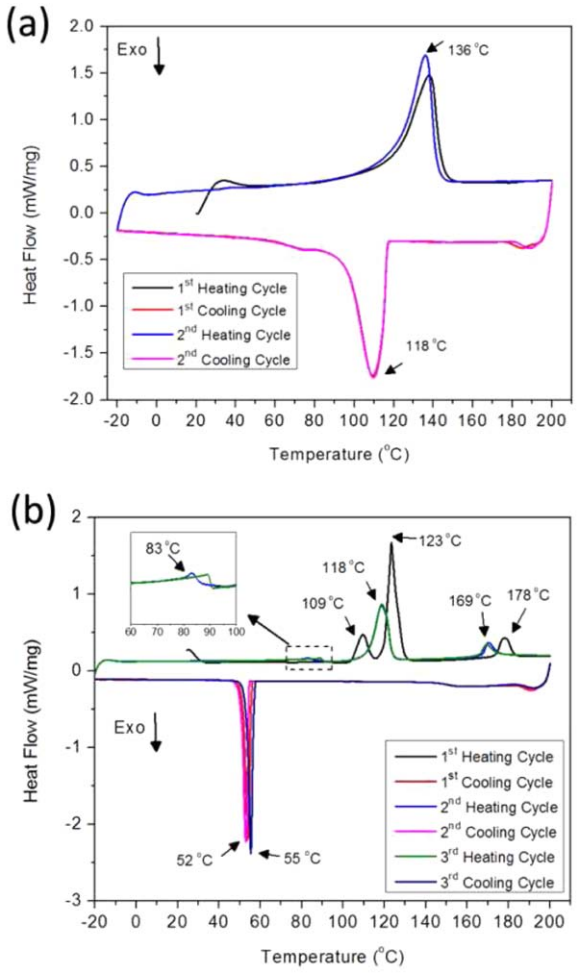

Figure 1. DSC traces of HDPE (a) and elemental sulfur (b). Major transitions are shown on the graph. [Color figure can be viewed in the online issue, which is available at wileyonlinelibrary.com.]

solid–liquid transition at ~115°C. Upon further heating, sulfur undergoes free radical ring opening polymerization at ~159°C and above. It is widely known that this polymeric form of sulfur is not stable and reverts back to S_8 at room temperature and pressure. If sulfur is to be used as filler for melt processed composites; these transitions are important to understand. HDPE has a melting point of 136°C. Hence, HDPE must be extruded at high temperature to form the composites. In this report, we have chosen a temperature of 190°C to extrude HDPE with elemental sulfur. At this temperature, HDPE will be in molten state while sulfur should be in polymeric form as discussed above. All composites were extruded without any processing complication such as viscosity mismatch between filler and host, plasticization effect, macrophase separation or aggregation. It is surprising that such issues were not observed even for sulfur loading as high as 30 wt %! Additionally, no H_2S has been detected during extrusion. Similarly, minimum SO_2 has been produced during extrusion because nitrogen was used as blanket to minimize sulfur oxidation. Detectors were used for both gases but none of them recorded any readings. But, composites have odor similar to SO_2, which probably were produced at concentration below detectors limits. In any case, when extruding sulfur, inert conditions must be used to avoid oxidation.

DSC Analysis

DSC was conducted on HDPE and elemental sulfur. Figure 1 Shows DSC traces for HDPE (a) and sulfur (b). Table I shows values of transition temperatures and enthalpies associated with each transition. HDPE shows single melting point at temperature of ~137°C, with an estimated enthalpy of melting of 113 J/g. Upon cooling, HDPE crystallizes at temperature ~118°C with enthalpy of crystallization of 113 J/g. The same is observed for both first and second heating-cooling cycles for HDPE.

Elemental sulfur shows three transitions in the first heating cycle and one transition in the first cooling cycle. In the first heating cycle, elemental sulfur undergoes solid-solid transition from orthorhombic crystal to monoclinic crystal at 109°C (enthalpy of 1 J/g) and with further heating, it undergoes melting at 123°C with enthalpy of melting of 30 J/g. With further heating, sulfur undergoes ring opening polymerization at ~178°C with enthalpy of polymerization of 3.4 J/g. But, when sulfur is cooled from that state, it undergoes a single sharp transition at ~52°C, well below all of the endothermic transitions. This peak should be assigned to a crystallization of polymeric sulfur. But, a typical crystallization exotherm for polymeric materials is rather broad. If this peak is for polymeric sulfur, it would mean that polymeric sulfur forms highly crystalline structure and/or have low polydispersity index. This is not the case because sulfur in the polymeric state is actually rich with several allotropes (linear and rings) with appreciable radical content.[15] Hence, this transition is either chemical in nature (depolymerization) or physical in nature. The former is less probable because the initial system is mixture of several allotropes of sulfur and probability of equal reactivity of all depolymerizing species (hence peak sharpness) is difficult to attain. The latter is more probable but requires that sulfur transforms into a single allotrope followed by crystallization from liquid to solid. This is possible but in the process it must have experienced super cooling because the exotherm temperature is way below the melting endotherm temperature (52°C vs. 123°C). However, it is reported in the literature that sulfur (predominantly S_8) cooled from the melt will crystalize into the beta-S_8 (monoclinic sulfur). This exotherm is then assigned to sulfur crystallization into the monoclinic S_8 despite the fact that this form melts at 123°C as discussed above. It is also possible that this transition is a vitrification, but we cannot confirm this at this stage.

In the second and third heating-cooling cycles, elemental sulfur show three endotherms and single exotherm. The first endotherm is minute and occurs at ~82°C (enthalpy <0.5 J/g) and is probably attributed to solid-solid transition. The second endotherm occurs at 118°C (enthalpy of ~37.4 J/g) and is attributed to melting transition of monoclinic sulfur followed by the third endotherm at 169°C (enthalpy of ~5 J/g), which is attributed to sulfur polymerization. It is worth mentioning that enthalpy of transitions in the second and third heating cycles for sulfur have different magnitude. For example, the melting endotherm is ~37 J/g in the second heating cycle compared to

Table I. Summary of DSC Results of HDPE and Elemental Sulfur

	HDPE		Sulfur	
	Transition temperature (°C)	Enthalpy of transition (J/g)	Transition temperature (°C)	Enthalpy of transition (J/g)
First heating cycle	137.9	114.3	109.6	1.0
			123.7	30.8
			178.1	3.4
Second heating cycle	136.1	112.5	82.9	<0.5
			118.5	37.4
			170.3	5.5
Third heating cycle			89.0	<0.5
			118.7	36.2
			169.4	5.0
First cooling cycle	118.2	114.3	52.0	28.5
Second cooling cycle	118.4	112.5	53.8	28.6
Third cooling cycle			55.5	29.6

~30 J/g in the first heating cycle. The same is true for the polymerization endotherm. Additionally, the temperature of these transitions shifted to lower values (melting occurred at 123°C in the first heating cycle compared to 118°C in the second and third). In the second and third cooling cycles, a single exotherm appears at ~53–55°C, similar to the single exotherm in the first heating-cooling cycle with similar magnitude for enthalpy (~28 J/g).

DSC results for HDPE-S composites are shown in Figure 2. All of the above sulfur transitions have not appeared in the HDPE-S composites except the melting temperature, which overlaps with HDPE melting transition. It is important to remember that DSC was conducted on composites after processing, which means that whatever the state of sulfur is, it would be due to the extrusion process. All composites have shown single transition in the heating cycle and single transition in the cooling cycle, with similar transition temperatures as HDPE. Hence sulfur has not significantly affected the melting and crystallization temperatures of HDPE (see Table II). Additionally, sulfur might have formed a polymeric allotrope (or probably other types of allotropes) when it was processed at 190°C and it retained this form when the composites were cooled from the melt because of absence of typical sulfur transitions that have been described above. From DSC we can conclude that: (1) typical transitions for orthorhombic sulfur (the typical crystal for S_8 allotrope) disappear; (2) polymerization temperature of elemental sulfur also disappear; (3) crystallization temperature of elemental sulfur also disappear; (4) HDPE transition temperatures have not changed or been affected by the presence of sulfur, which led us to conclude that sulfur is predominantly present in the amorphous phase of HDPE. If we examine the enthalpy of melting of the composite compared to a theoretical enthalpy of melting (Table II), we observe that the theoretical values are less than the experimental values. In other word, if we assume that elemental sulfur (in its S_8 allotrope) and HDPE form a physical mixture, the melting enthalpy of the mixture will follow additivity rule. In our case, the additivity rule failed to reproduce the experimental value of the composite. Hence, sulfur is not in its orthorhombic crystal structure. The difference has to be due to other allotrope of sulfur or a different S_8 crystal (monoclinic for

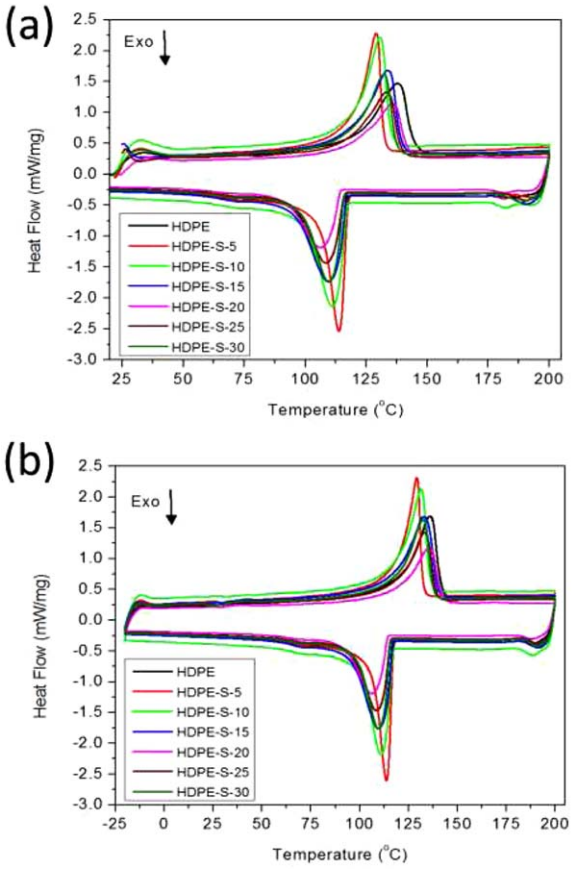

Figure 2. DSC traces for HDPE-S composites showing the melting endotherms and crystallization exotherms. First heating-cooling cycle is shown in (a) and the second heating-cooling cycle is shown in (b). [Color figure can be viewed in the online issue, which is available at wileyonlinelibrary.com.]

Table II. Summary of Results Obtained from DSC Analysis for HDPE-S Composites

Sample code	HDPE-S-5	HDPE-S-10	HDPE-S-15	HDPE-S-20	HDPE-S-25	HDPE-S-30
T_m (°C, experiment)	129.3	131.8	132.8	133.3	133.1	130.9
ΔH_m (J/g, experiment)	107.5	107.9	108.2	109.1	109.1	105.9
ΔH_m (J/g) [Theoretical using values for pure S_8 data in this report at $T = 123.7$°C in the first heating cycle]	110.1	105.95	101.7	97.6	93.4	89.2
ΔH_m (J/g) [Theoretical using values for pure S_8 data in this report at $T = 118$°C in the second and third heating cycle]	110.4	106.5	102.7	98.8	94.9	91.1
ΔH_m (J/g) [Theoretical using polymeric sulfur enthalpy of melting][20]	112.1	111.8	111.4	111.1	110.8	110.4
T_c, (°C, experiment)	110.3	111.1	110.8	111.6	111.7	109.5
ΔH_c (J/g, experiment)	110.2	110.8	107.5	107.7	107.7	99.7
ΔH_c (J/g) [Theoretical using values for pure S_8 data in this report at $T \sim 53$°C]	109.2	105.0	100.8	96.5	92.3	88.1

example). The latter hypothesis is not supported by the experimental values of the enthalpy of melting. That is, if sulfur is in its S_8 allotrope with monoclinic crystal structure, then the enthalpy of melting of the composites would have been 91 J/g for composite with 30 wt % sulfur loading. But the experimental value for the composite is 105 J/g. If sulfur exists as a polymer,[20] then the theoretical value of this enthalpy would be 110 J/g. Hence, the most probable allotrope of sulfur in the composite is mixture of polymeric sulfur and S_8. But in the Raman analysis (see below), polymeric sulfur was not detected. Therefore sulfur is present in S_8 allotrope but in a structure that is not well understood, an amorphous structure is also possible due to crystallization hindrance from the presence of HDPE chains. It was observed that values of melting temperature (T_m), enthalpy of melting (ΔH_m), crystallization temperature (T_c), and enthalpy of crystallization (ΔH_c) all decreased on addition of sulfur. The drop is not significant and is attributed to the effect of lack of interaction between sulfur and crystalline domain of HDPE and restriction on the segmental chain movement of HDPE upon cooling, which is imposed by the presence of sulfur.[21,22]

FTIR Analysis

To confirm the presence of HDPE, composites were characterized by using FTIR-ATR. IR bands in Figure 3 are in good agreement with those reported in the literature for high density polyethylene.[23,24] The IR peaks at 2914, 2852, 1462, and 717 cm^{-1} are attributed to methylene (—CH_2—) nonsymmetric stretching vibration, methylene symmetric stretching vibration, methylene nonsymmetric changing angle vibration (scissoring) and methylene swing in plane vibration (rocking), respectively. The spectra of modified and unmodified sulfur composites show absorption peaks in the range of 1115–1250 cm^{-1} are attributed to the C—H bending vibration (twisting). The spectra of HDPE-S composites are almost identical to that of HDPE, which confirms that sulfur does not affect the chemistry of HDPE. The FTIR-ATR spectra of HDPE-S composites confirm

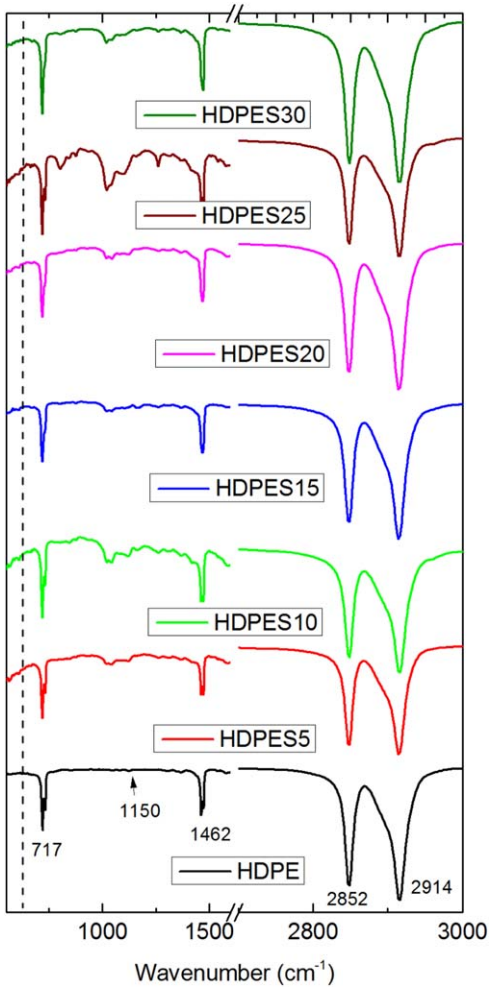

Figure 3. FTIR spectra of HDPE and HDPE-S composites. [Color figure can be viewed in the online issue, which is available at wileyonlinelibrary.com.]

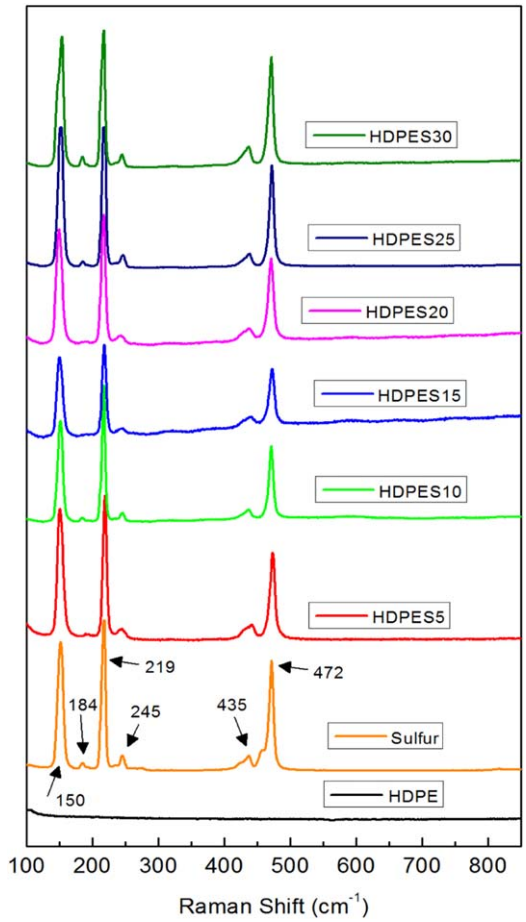

Figure 4. Raman spectra of HDPE, sulfur, and HDPE-S composites in the spectral range 100–600 cm^{-1}. [Color figure can be viewed in the online issue, which is available at wileyonlinelibrary.com.]

that no band at 620 cm^{-1} is observed for C—S bond (dashed line in Figure 3), indicating that sulfur and HDPE didn't undergo any chemical reaction, which is a key finding and is desirable in this composite system. Hunter *et al.*[25] reported that C—C and C—H bonds are stronger bond and requires high energy (348 and 410 kJ/mol)[26] to break. Bond breakage did not occur during extrusion as the breaking of C—C and C—H bonds require high temperature, high pressure or the presence of catalyst,[27] none of which were present in the melt mixing process within the extruder.

Raman Analysis

Raman spectroscopy was used to examine the composite system at the molecular level and evaluate the intermolecular interactions. Figures 4–6 show Raman spectra of HDPE, sulfur and HDPE-S composites at different ranges. The elemental sulfur has been well identified by its Raman bands at 150 (s), 184 (w), 219 (s), 245 (w), 435 (w), and 472 (s) cm^{-1}, respectively. The letters (w), (s) stand for weak and strong Raman bands. Raman results are in agreement with previous reports.[27,28] These bands confirm that elemental sulfur exists in the composites in cyclo-octasulfur allotrope. It would seem that DSC results and Raman results are contradictory. However, DSC shows that sulfur is not in its orthorhombic crystal, which does not imply that sulfur is not in an S_8 allotrope. In other words, sulfur still exists as S_8, but not in its orthorhombic crystal. Monoclinic or even amorphous form is plausible. Moreover, it is known polymeric sulfur has broad Raman lines around 460 cm^{-1}, which have not been detected in these composites despite the fact that processing conditions are indeed above polymerization temperature. Raman spectrum of the incorporated HDPE-S films do not show any new peak at 789 cm^{-1}, which would be expected if a reaction between sulfur and carbon occurred. This confirms that sulfur did not undergo a reaction with HDPE in agreement with ATR-FTIR results.

Raman spectra for all samples in the band zones (1000–1600 cm^{-1}) of HDPE were expanded in order to facilitate the identification of the peaks of amorphous and crystalline phases in Figure 5. Peaks at 1062 and 1129 cm^{-1} can be attributed to the C–C stretching bond of all-trans-$(CH_2)_n$- while peak at 1081 is attributed to amorphous phase of HDPE. It has been previously reported that peaks at 1056 cm^{-1}, 1079, 1125 cm^{-1} can be attributed to the carbon (C-C) vibration of polyethylene crystallites.[29–31] Peaks at 1062 and 1127 cm^{-1} are present with similar intensities in all composites, which suggests that the crystalline phase vibration is not influenced by sulfur atoms. C-C stretching for the amorphous phase is at 1081 cm^{-1} and this

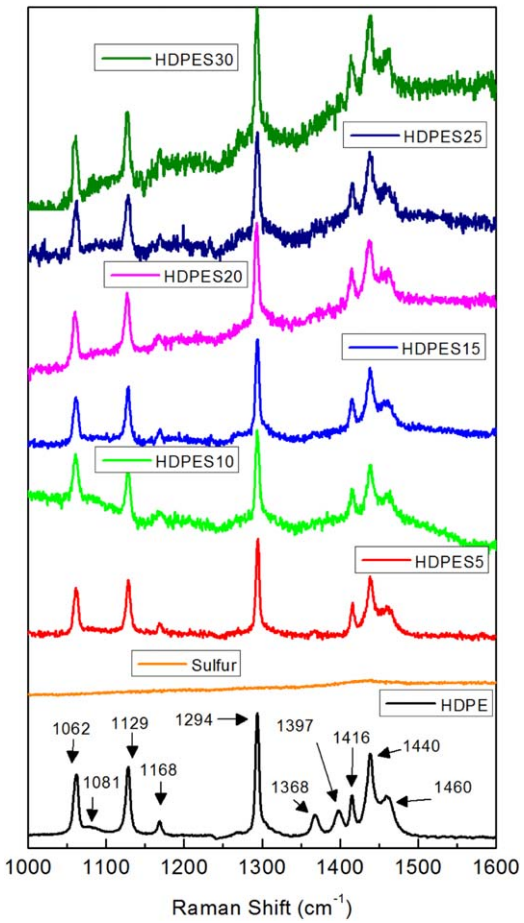

Figure 5. Raman spectra for HDPE, sulfur, and HDPE-S composites in the 1000–1600 cm^{-1} range. [Color figure can be viewed in the online issue, which is available at wileyonlinelibrary.com.]

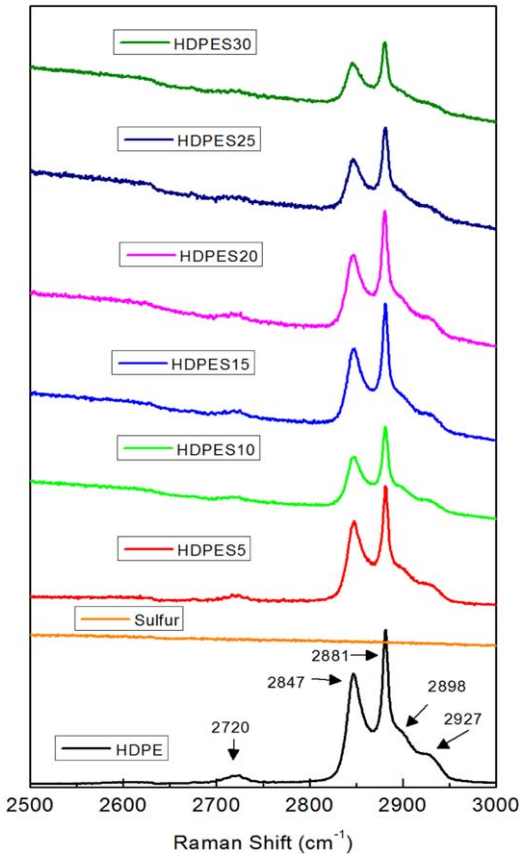

Figure 6. Raman spectra for HDPE, sulfur, and HDPE-S composites in the 2500–3000 cm^{-1} range. [Color figure can be viewed in the online issue, which is available at wileyonlinelibrary.com.]

one disappears when sulfur was added, which means that sulfur is predominately distributed in the amorphous phase of HDPE and it suppresses this subtle Raman band. Additionally, composites display the bending absorption peaks at 1460 cm^{-1} [asymmetric $\delta(CH_3)$ bending band], 1440 cm^{-1} [asymmetric $\delta(CH_2)$ bending band], 1416 cm^{-1} [symmetric $\delta(CH_2)$ bending band], and 1397 cm^{-1} [symmetric $\delta(CH_3)$ bending band], respectively. In addition to the bending vibrations of the individual identities of HDPE, the absorption bands at 1368, 1294, and 1168 cm^{-1} were due to the CH_3 wagging, CH_2 twisting and CH_2 rocking, respectively. Two peaks have disappeared in the composites, 1397 (symmetric CH_3 bending) and 1368 (CH_3 wagging). Therefore sulfur interacts strongly with these methyl groups to suppress this Raman mode. But, no chemical bond formed in the process. If it did, it means the composites will have thiol groups[3] and C═C bonds, neither have been detected using Raman. Figure 6 shows Raman spectra in the 2500–3000 cm^{-1} range. Peaks at 2720, 2847, 2881, 2898, and 2927 cm^{-1} are assigned to the various vibrational modes for CH_2 group. The presence of sulfur has not led to major changes in these modes and a typical band for thiol at 2550–2600 cm^{-1} is not observed, which confirms the absence of reaction between sulfur and HDPE. Taken in combination with the FTIR data, it can be concluded that sulfur molecules have not chemically linked to the carbon matrix of HDPE and it is spatially distributed in the amorphous phase of HDPE.

XRD Analysis

Figures 7 and 8 show the diffraction profiles of elemental sulfur, HDPE and HDPE-S composites. Elemental sulfur showed typical characteristic diffraction peaks located at 23.1, 25.9, 27.8, and 28.6° indicating crystallized orthorhombic sulfur (S_8) structure.[32] This crystallized orthorhombic sulfur was disturbed in the composite as shown in the figures. HDPE is characterized by two broad standard diffraction peaks at 21.8° (110) and 24.2° (200).[33,34] Diffraction of HDPE-S show two features; the first is the shift of the (110) and (200) peaks of HDPE to slightly higher angle (and hence lower d-spacing) at moderate sulfur loading and it returns to higher angle with higher sulfur loading. Secondly, the predominant sulfur peak (at 2θ ~23.1 for the orthorhombic crystal) disappears at moderate sulfur loading and it appears again at higher sulfur loading but at slightly higher angle (23.1 vs. 23.6), which implies lower d-spacing. The diffraction peaks found for HDPE, elemental sulfur and HDPE-S are summarized in Table III in comparison with reported XRD results for polymeric sulfur.[20,35] By comparing these together, it can be

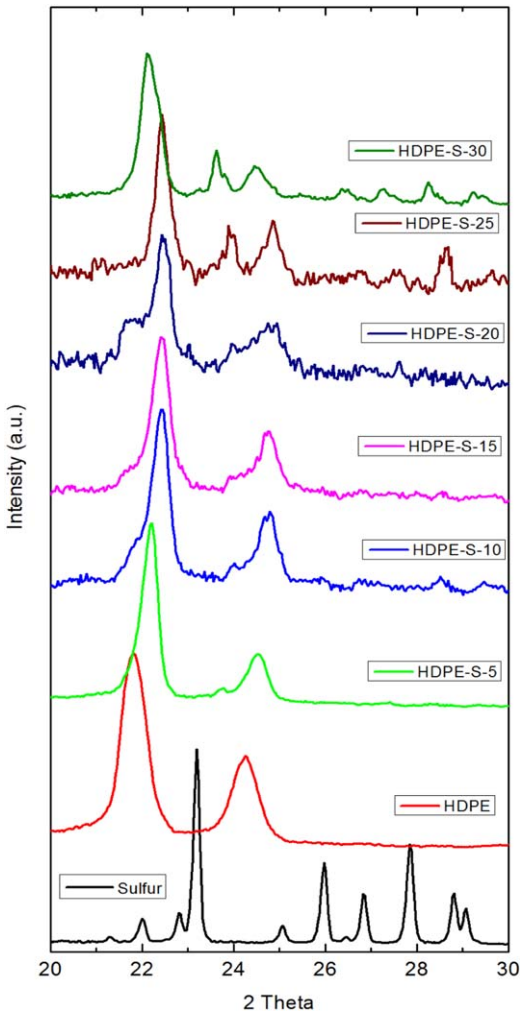

Figure 7. X-ray diffraction patterns for sulfur, HDPE, and HDPE-S composites in the range of 20–30 (2 theta). [Color figure can be viewed in the online issue, which is available at wileyonlinelibrary.com.]

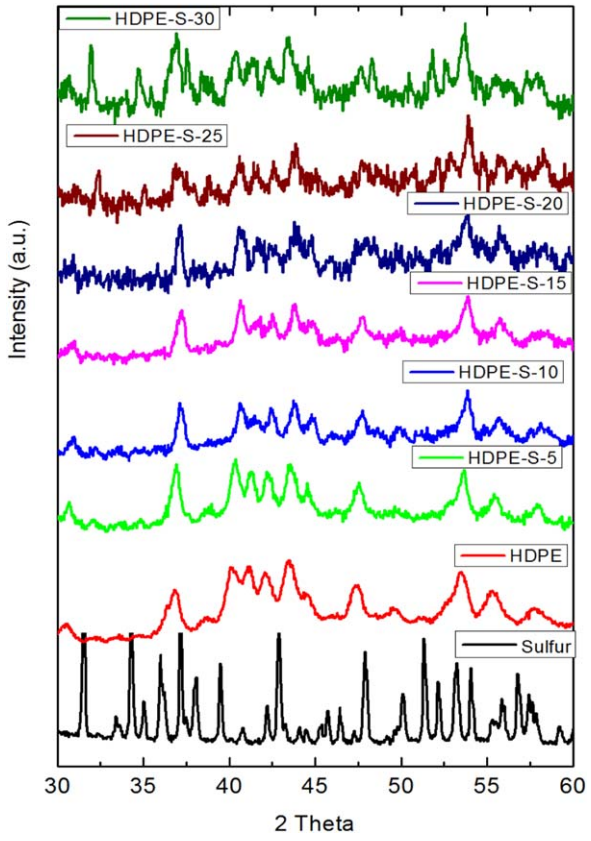

Figure 8. XRD patterns of HDPE, elemental sulfur, and HDPE-S composites in the range of 30 to 60 (2 Theta). [Color figure can be viewed in the online issue, which is available at wileyonlinelibrary.com.]

concluded that polymeric sulfur did not form in the composite, nor did sulfur crystalized into the orthorhombic crystal (except at high loading).

TEM Analysis

TEM images are used to visually assess sulfur dispersion within the polymer matrix. Figure 9 shows TEM images of the composite samples at different sulfur loading. The best dispersion of sulfur is seen in the HDPE-S-5 and HDPE-S-10 samples and the poorest dispersion is seen in the HDPE-25 and HDPE-S-30 sample where the appearance of darkly contrasted and parallel edges is indicative of multilayer sulfur aggregates. Similar dark edges are also seen in the HDPE-S-10, HDPE-S-15, and HDPE-S-20 composite samples, but the more diffuse coloration suggests better separation and more evenly oriented sulfur layers than in high sulfur content sample. These analyses can be drawn about the homogeneity of sulfur in composite materials. Although it is quite convenient to make conclusive statements from the TEM images, it seems that many of the sulfur in composites have elongated shapes. These findings can be understood as a sulfur growth mechanism in which the HDPE matrices restrict the decrease in surface area that typically accompanies sulfur coalescence. HRTEM images shown in Figure 10 accurately illustrate the transition from discrete sulfur particles to a composite structure. This finding also highlight a further advantage of synthesizing route in that these composite materials are homogeneous and the phase mixing induced by thermal processing allows precise control over the sulfur dimensions in the resulting composites.

SEM Analysis

Scanning electron microscopy imaging (Figure 11) of HDPE-sulfur composites reveals homogeneous distribution of sulfur particles within polymer matrix. Intense extrusion results in effective sulfur dispersion and successfully prevents agglomeration, so well-separated individual sulfur particles predominate in filler phase. Noticeable differences in morphology of composites depending on elemental sulfur loading are observed. Thus, the low elemental sulfur loading (5 wt %) sample demonstrates

Table III. XRD Data of HDPE, Elemental Sulfur, and HDPE-S Composites and Reported Data for Polymeric Sulfur

Sample name	Peak Position (2θ)	d-spacing (Å)	Sample name	Peak Position (2θ)	d-spacing (Å)	Sample name	Peak Position (2 θ)	d-spacing (Å)
HDPE	21.80	4.07	HDPE-S-10	22.36	3.97	HDPE-S-25	22.42	3.96
				24.70	3.60			
						23.92	3.71	
	24.21	3.67				24.82	3.58	
Elemental Sulfur	23.17	3.83	HDPE-S-15	22.37	3.97	HDPE-S-30	22.15	4.00
				24.71	3.60			
						23.62	3.76	
	25.94	3.43				24.48	3.63	
	27.82	3.20						
HDPE-S-5	22.13	4.01	HDPE-S-20	22.40	3.96	Polymeric sulfur[20]	22.22	4.06
				24.71	3.60			
						25.55	3.85	
	24.49	3.63				29.44	3.08	

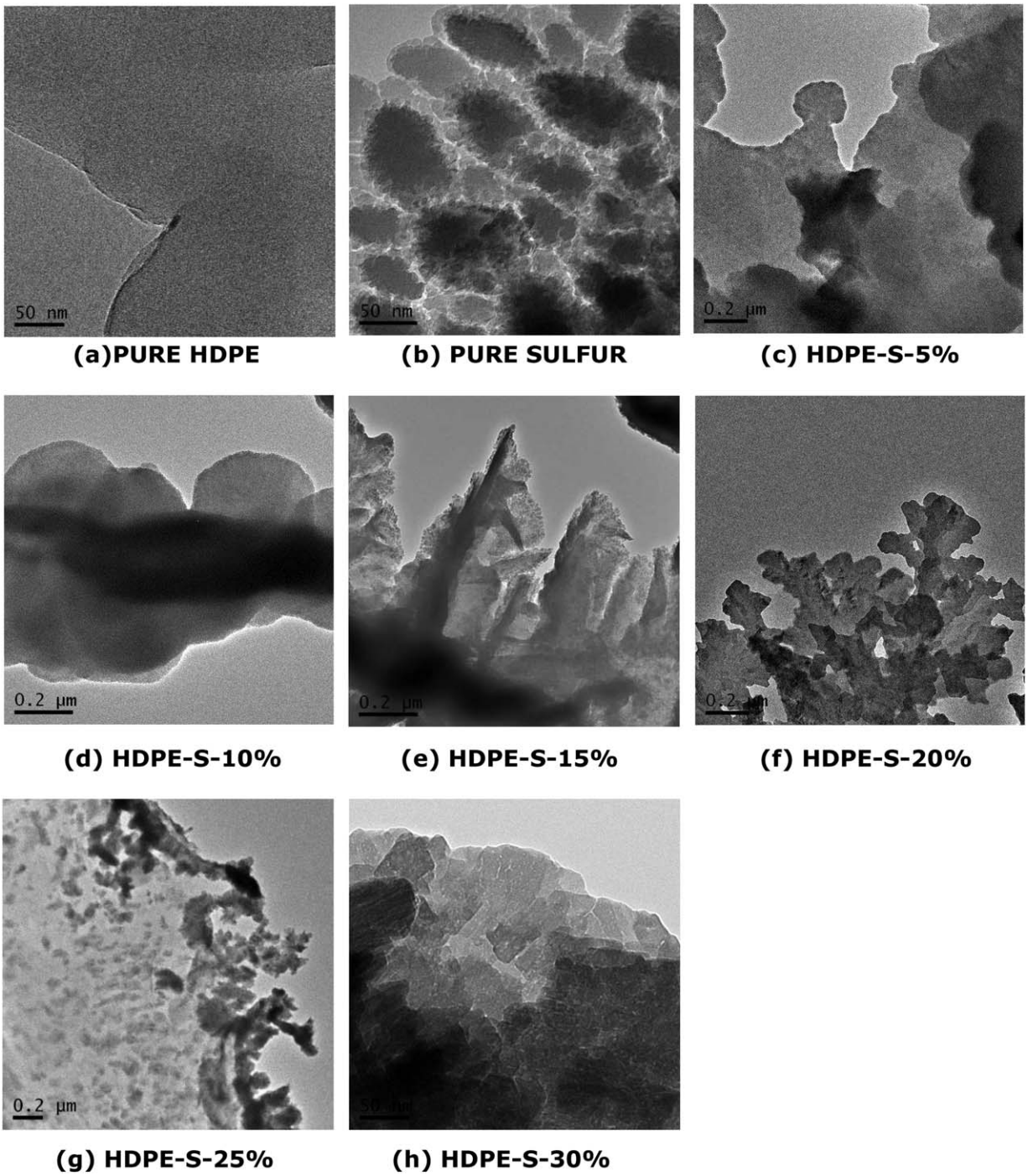

Figure 9. Representative TEM images of pure sulfur, pure HDPE, and HDPE-S composites.

the most efficient HDPE reinforcement. Sulfur is perfectly covered with HDPE shell and strongly embedded in the polymer matrix that displays very good interfacial adhesion. On increasing the sulfur content, we observe the sulfur particles are partly aggregated which evidence the decrease of interfacial adhesion in the composite material. Sulfur particles aggregation becomes predominant at high elemental sulfur loadings that signify considerable deterioration of sulfur reinforcement efficiency in composite.

TGA Analysis

Thermo-gravimetric analysis (TGA) was used to determine hybrid material thermal stability and its volatile components fraction by monitoring the weight change with temperature. The thermogravimetry analysis curves for the HDPE, elemental sulfur and HDPE-S hybrid composite samples with various amount of elemental sulfur are shown in Figure 12 and 13 and summary is available in Table IV. From the TGA study of pure sulfur, degradation starts at ~229°C because sulfur bonds are

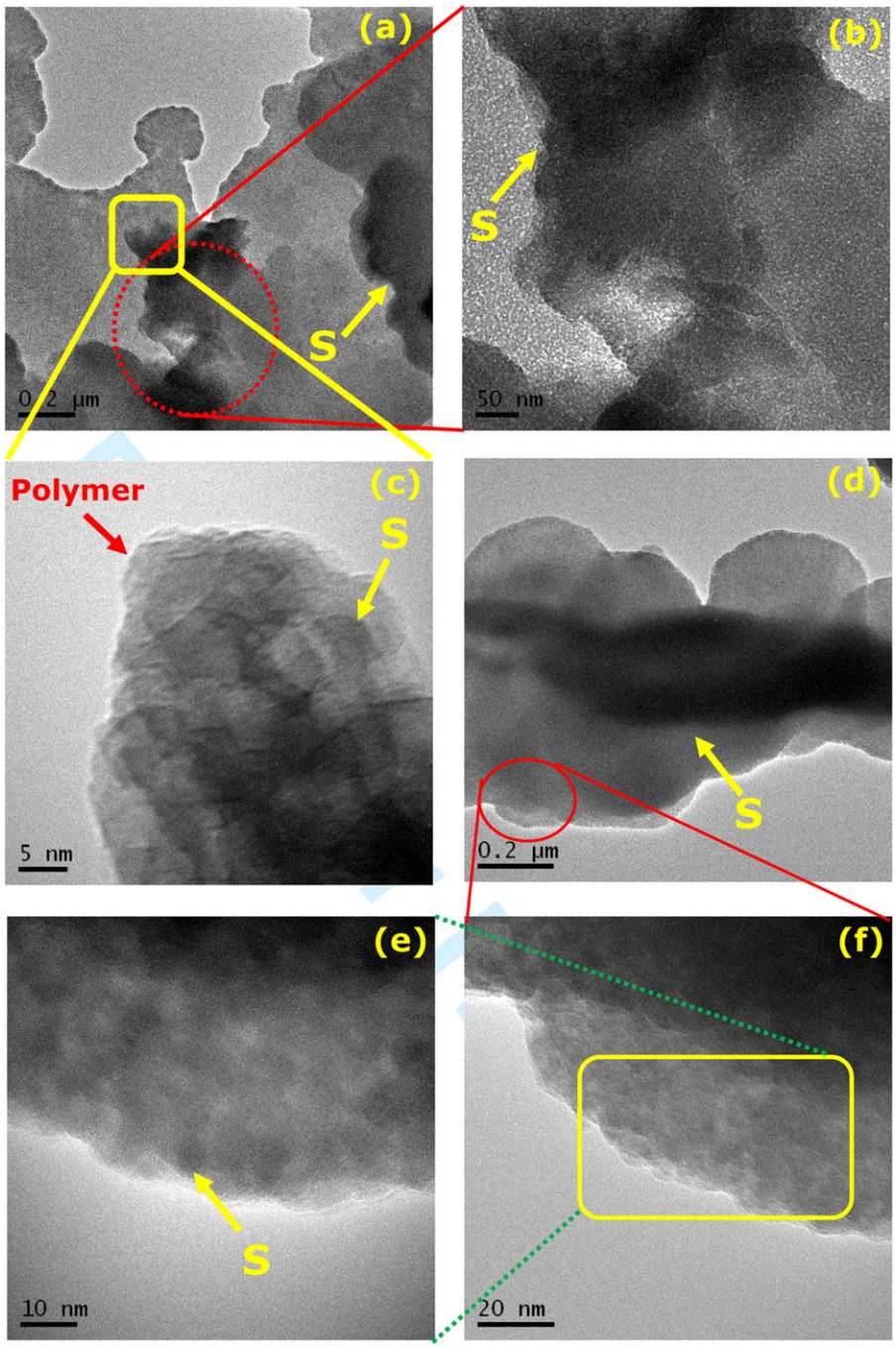

Figure 10. Representative HRTEM images of sulfur composites; (a) HDPE-S-5% (b) expanded zone(c) expanded zone of second area (d) HDPE-S-10% (e)and (f) expanded zone of S-10% composite. Expanded zone shows significant fluctuations in the size, morphology and distribution of the sulfur in the hybrid composites. [Color figure can be viewed in the online issue, which is available at wileyonlinelibrary.com.]

relatively weak and this sets the upper processing temperature above which sulfur degrade. For pure HDPE, degradation starts at 437°C. TGA for Composites showed that sulfur initial degradation temperature was shifted to slightly higher temperatures (Table IV). A major weight loss, starts at 420°C which end approximately at 500°C depending on sulfur composition. It is the main degradation occurred to the structure of HDPE[21,22,36] indicating the initiation of a second degradation zone. A slow further loss of weight occurred until 900°C, indicating that there is further reaction involving char. In this study, three major constituents of composite materials are chemically active and decomposes thermally in the temperature range of 100–500°C (volatile component decomposes mainly between 100 and 110°C, sulfur decomposes between 200 and 300°C and HDPE undergoes decomposition between 400 and 500° C). From the above TGA study it shows that the most suitable processing temperature for HDPE-S before the sulfur degrades is below 200°C.

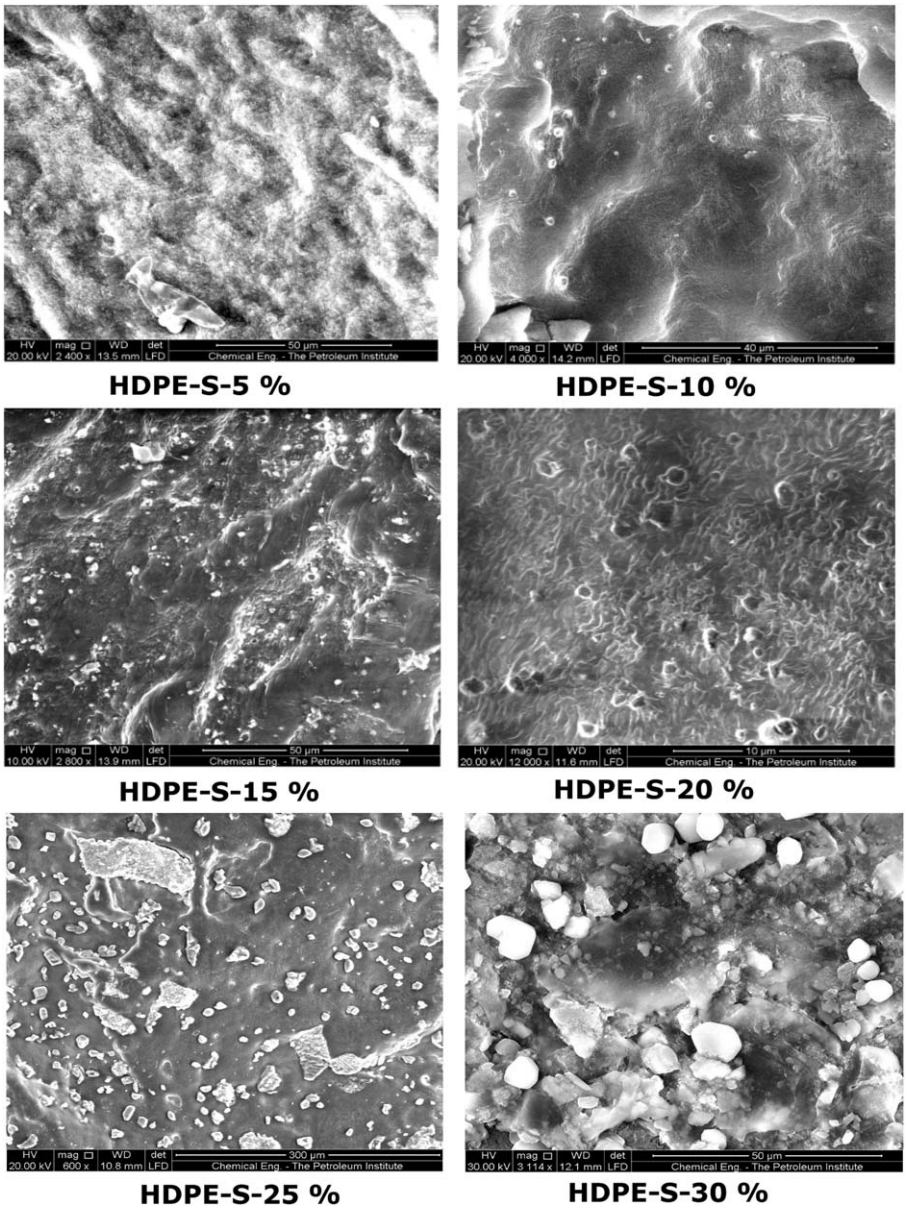

Figure 11. SEM image of HDPE-sulfur based composites.

Mechanical Properties

The modulus values, elongation percentage (%) and ultimate tensile strengths (UTS) of pure HDPE and sulfur/HDPE composites are presented in Figure 14 and Table V. The young modulus values of composites decreases with increasing sulfur loading. Sulfur incorporation has considerable impact on composite tensile properties; noticeable Young's modulus decreases from 673 to 556 MPa takes place at 5 wt % sulfur loading, and further modulus decreases with sulfur loading (Table V). This might be observed due to weak physical bonds between sulfur and polymer. The mechanical properties were fluctuated more at high sulfur loading composites. The reason for the fluctuating properties at high sulfur concentration is due to the uneven mixing of sulfur-HDPE. The composite used for testing, the sulfur is not evenly distributed and this leads to some stronger and some weaker parts which result the tensile properties of the samples went up and down. The tensile strength of the composites increases with increasing content of elemental sulfur is shown in Table V and Figure 14. This could be attributed to the strong interfacial adhesion between both phases sulfur and polymer, resulting less de-bonding of the matrix from the sulfur network during the tensile deformation. The de-bonding results in void formation, which lowers the tensile strength because cracks can easily propagate through regions containing the voids but in this study, the HDPE-sulfur composites shows better tensile strength, which shows debonding effect was not strong in this composite. Mechanical results depend on consistent processing of the composites that can lead to uniform dispersion of the sulfur in the composites and eventually higher the tensile strength. Figure 14 shows tensile strain (elongation percentage) of pure HDPE and HDPE-sulfur composites. Generally, the addition of reinforcement materials reduces the tensile strain of

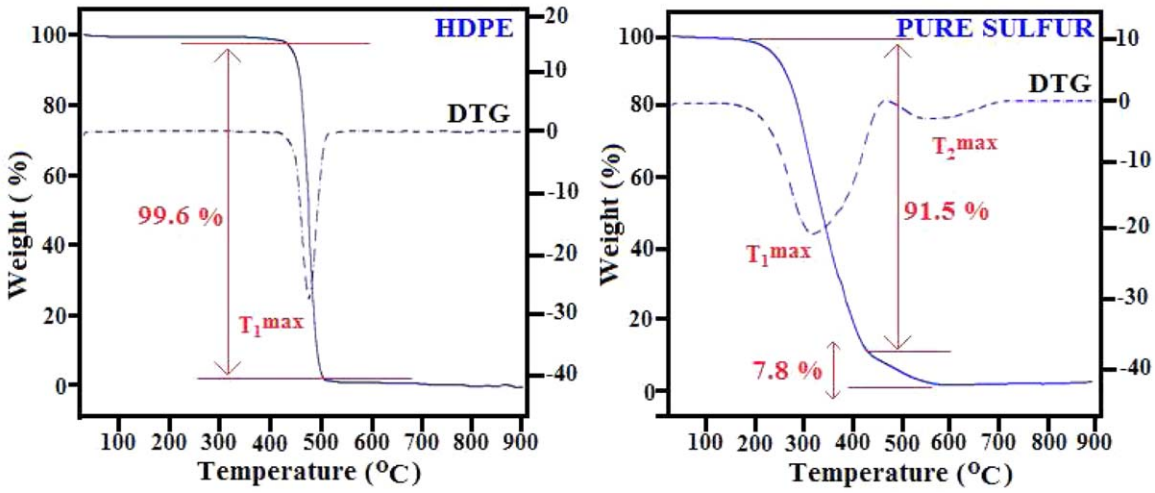

Figure 12. Thermogravimetric analysis (TGA) of HDPE and sulfur. [Color figure can be viewed in the online issue, which is available at wileyonlinelibrary.com.]

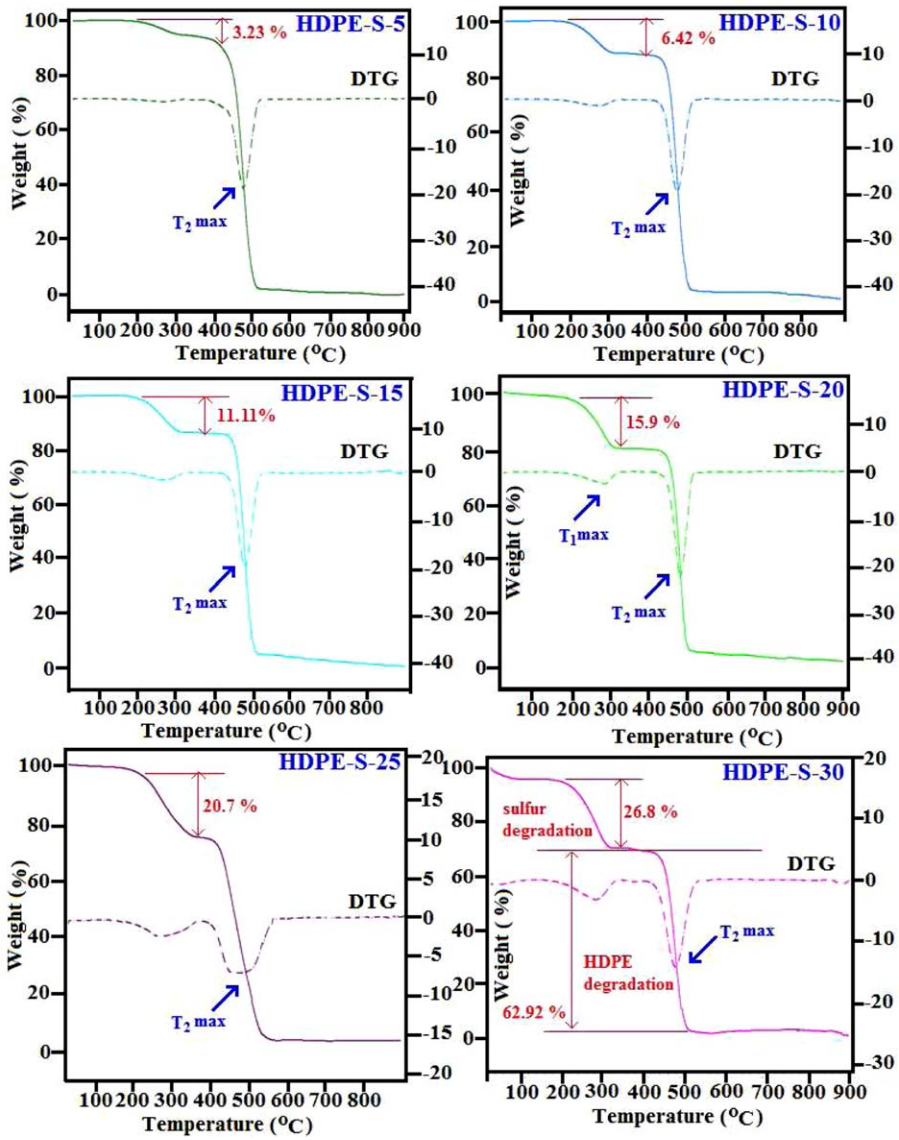

Figure 13. TGA curves for HDPE-S composites. [Color figure can be viewed in the online issue, which is available at wileyonlinelibrary.com.]

Table IV. TGA Parameters of HDPE, Sulsur, and HDPE-S Composites

Sample code	T_1on (°C)	T_1max (°C)	T_1end (°C)	T_2on (°C)	T_2max (°C)	T_2end (°C)	Residual (wt. %) 500°C	550°C	600°C
HDPE	437.8	474.5	504.1	—	—	—	7.32	6.13	3.40
Sulfur	229.4	320.6	421.7	499.7	563.9	627.3	2.85	0.88	0.84
HDPE-S-5	229.9	271.8	304.8	424.5	471.7	505.2	8.13	2.69	2.29
HDPE-S-10	232.0	272.4	306.3	437.7	473.6	508.1	10.17	3.13	3.02
HDPE-S-15	233.2	273.1	309.6	438.9	478.5	509.7	10.21	3.33	3.13
HDPE-S-20	233.5	275.9	309.8	444.1	479.2	510.2	13.11	5.23	4.56
HDPE-S-25	232.9	294.1	337.3	412.3	480.9	540.6	16.13	6.94	6.16
HDPE-S-30	231.8	280.4	321.2	416.8	481.1	539.3	15.67	6.05	4.23

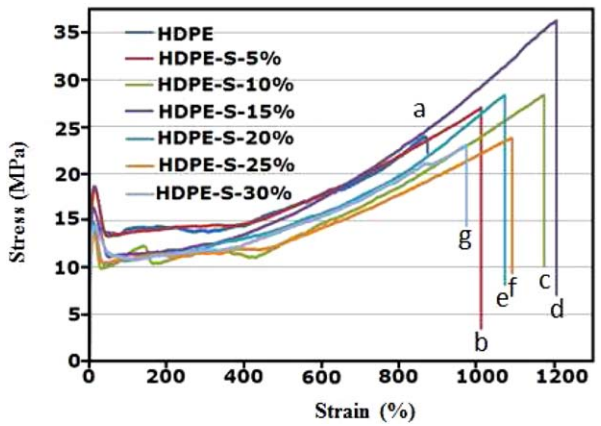

Figure 14. Stress–strain graph of S-HDPE based composites: (a) HDPE; (b) HDPE-S-5%; (c) HDPE-S-10%; (d) HDPE-S-15%; (e) HDPE-S-20%; (f) HDPE-S-25% and (g) HDPE-S-30%. [Color figure can be viewed in the online issue, which is available at wileyonlinelibrary.com.]

composites. But in this study, the tensile strain of the composites is higher compared to pure HDPE and greatly increases with sulfur loading. The elongation probably arises from the sulfur because the HDPE is rigid relative to sulfur. Decreasing the amount of polymer increases the amount of sulfur available for the elongation. A small decrease in tensile, elongation and modulus can be observed for composites with 25 and 30% of sulfur. Some variation was observed in high sulfur concentration composites due to not so good dispersion of sulfur, as already mentioned and shown in TEM and SEM (Figures 9 and 11). Better mechanical performance of 5, 10, and 15% sulfur in the composites was studied in this work. This suggests that this material may have better dispersion of sulfur than the composites containing 25 and 30% of the same material, which showed lower strength values.

Table V. Elongation (%), UTS (MPa), and Modulus (MPa) of HDPE-Sulfur Composites

Sample name	Elongation (%)	UTS (MPa)	Modulus (MPa)
HDPE	835 ± 54	22.6 ± 4	673 ± 122
HDPE-S-5%	1011 ± 14	24.6 ± 2.5	556 ± 40
HDPE-S-10%	1110 ± 45	26.8 ± 1	558 ± 26
HDPE-S-15%	1202 ± 29	29.4 ± 6	631 ± 105
HDPE-S-20%	1096 ± 156	29.14 ± 6	668 ± 8
HDPE-S-25%	1048 ± 56	22 ± 2.9	543 ± 40
HDPE-S-30%	932 ± 77	22.25 ± 2.7	638 ± 15

CONCLUSIONS

This work shows for the first time; the use of elemental sulfur in composite formulations with no cross-reaction with host matrix. Composites were prepared using extrusion at temperature above sulfur polymerization temperature. Processing of sulfur and HDPE proceeded without complication and without the need for modifications of either constituent. Sulfur loading up to 30 wt % was achieved. Calorimetry showed that crystallinity fraction of HDPE has not changed and sulfur is present in the composite in non-orthorhombic crystal form of S_8. Spectroscopy confirmed the absence of chemical bonds between sulfur and HDPE and the presence of predominantly S_8 allotrope. XRD confirms the absence of orthorhombic crystal but didn't confirm the presence of polymeric sulfur. We conclude that sulfur retains its S_8 allotrope but not in orthorhombic crystal and polymeric sulfur is not present in the composites despite the fact that processing was done above polymerization temperature. Mechanical testing revealed increasing in elongation at break and ultimate strength while Young's modulus decrease as a result of sulfur addition. This is an indication of a plasticization effect of sulfur on HDPE. The present study opens the door for further research on sulfur as filler in composite materials.

ACKNOWLEDGMENTS

This work is funded by the Gas Subcommittee of Abu Dhabi National Oil Company (ADNOC) Research & Development. We thank Samuel Stephen for his help in TEM imaging.

REFERENCES

1. Dogadkin, B. A.; Dontsov, A. A. *Polym. Sci. U.S.S.R.* **1962**, *3*, 1107.
2. Dogadkin, B. A.; Dontsov, A. A. *Polym. Sci. U.S.S.R.* **1965**, *7*, 2021.

3. Douglas, A. O.; Jean Osteraas, A. *J. Polym. Sci. Part A: Polym. Chem.* **1969**, *7*, 1913.
4. Chung, W. J.; Griebel, J. J.; Kim, E. T.; Yoon, H.; Simmonds, A. G.; Ji, H. J.; Dirlam, P. T.; Glass, R. S.; Wie, J. J.; Nguyen, N. A.; Guralnick, B. W.; Park, J.; SomogyiÁrpád Theato, P.; Mackay, M. E.; Sung, Y.-E.; Char, K.; Pyun, J. *Nat. Chem.* **2013**, *5*, 518.
5. Angelici, R. J. *Acc. Chem. Res.* **1988**, *21*, 387.
6. Sandrolini, F.; Manzi, S.; Andrucci, A. *Composites: Part A* **2006**, *37*, 695.
7. Paulson, J. E.; Simic, M.; Campbell, R. W. *J. Am. Chem. Soc.* **1978**, 215.
8. Mohamed, A. M. O.; El-Gamal, M. M. *Environ. Geol.* **2007**, *53*, 159.
9. (a) Bourne, D. J. New Uses of Sulfur, II; American Chemical Society: Washington, **1978**; p ix, 282 p; (b) West, J. R. New Uses of Sulfur; American Chemical Society: Washington, **1975**; p x, 236 p.
10. Yin, Y. X.; Xin, S.; Guo, Y. G.; Wan, L. J. *Angew. Chem. Int. Ed.* **2013**, *52*, 13186.
11. (a) Griebel, J. J.; Namnabat, S.; Kim, E. T.; Himmelhuber, R.; Moronta, D. H.; Chung, W. J.; Simmonds, A. G.; Kim, K. J.; van der Laan, J.; Nguyen, N. A.; Dereniak, E. L.; Mackay, M. E.; Char, K.; Glass, R. S.; Norwood, R. A.; Pyun, J. *Polym. Adv. Mater.* **2014**, *3*, 3014; (b) Simmonds, A. G.; Griebel, J. J.; Park, J.; Kim, K. R.; Chung, W. J.; Oleshko, V. P.; Kim, J.; Kim, E. T.; Glass, R. S.; Soles, C. L.; Sung, Y. E.; Char, K.; Pyun, J. *ACS Macro Lett.* **2014**, 229.
12. Meyer, B. *Chem. Rev.* **1976**, *76*, 367.
13. Fujimori, T.; Morelos-Gomez, A.; Zhu, Z.; Muramatsu, H.; Futamura, R.; Urita, K.; Terrones, M.; Hayashi, T.; Endo, M.; Hong, S. Y.; Choi, Y. C.; Tomanek, D.; Kaneko, K. *Nat. Commun.* **2013**, *4*, 2162.
14. Liu, G.; Niu, P.; Yin, L.; Cheng, H. M. *J. Am. Chem. Soc.* **2012**, *134*, 9070.
15. Meyer, B. *Reviews* **1964**, *64*, 429.
16. Steudel, R. Elemental Sulfur and Sulfur-Rich Compounds I. Springer Verlag: Heidelberg, **2003**; p 230.
17. Rauchfuss, T. *Nat. Chem.* **2011**, *3*, 648648.
18. Trofimov, B. A. *Sulfur Rep.* **2003**, *24*, 283.
19. Schmidt, M. *Angew Chem. Int. Ed. Eng.* **1973**, *12*, 445.
20. Cataldo, F. *Angew Makromol. Chem.* **1997**, *249*, 137.
21. Ishidi, E. Y.; Adamu, I. K.; Kolawale, E. G.; Sunmonu, K. O.; Yakubu, M. K. *J. Emerging Trends Eng. Appl. Sci.* **2011**, *2*, 346.
22. Mendes, L. C.; Cestari, S. P. *Ind. Waste Mater. Sci. Appl.* **2011**, *2*, 1331.
23. Dalai, S.; Wenxiu, C. *J. Appl. Polym. Sci.* **1996**, *62*, 75.
24. Ioan, J. Z. L. N.; Q. W. *Compos. Int.* **2005**, *12*, 125.
25. Hunter, K. C. H.; East, A. L. L. E. *J. Phys. Chem. A* **2002**, *106*, 1346.
26. Stephen, J. B.; Ellison, G. B. *Acc. Chem. Res.* **2003**, *36*, 255.
27. Jae-Kwang Kim, X. Z.; Kwon, H.-J. A.; Jou, K. C. H. A. *Electrochim. Acta* **2013**, *109*, 145.
28. Ward, A. T. *J. Phys. Chem.* **1968**, *72*, 4133.
29. Colomban, P. *Adv. Eng. Mater.* **2002**, *4*, 535.
30. Galiotis, C. R.; Young, J.; Yeung, P. H. J.; Batchelder, D. N. *J. Mater. Sci.* **1984**, *19*, 3640.
31. Gouadec, G.; Karlin, S.; Colomban, P. *Compos. Part B* **1998**, *29*, 251.
32. Rettig, S. J.; Trotter, J. *Acta Cryst.* **1987**, *43*, 2260.
33. Leni, M. M. A. *J. Polym. Res.* **2008**, *15*, 83.
34. Minick, J.; Moet, A.; Baer, E. *Polymer* **1995**, *36*, 1923.
35. Tuinstra, F. *Physica* **1967**, *34*, 113.
36. Chowdhury, S. R.; Sabharwal, S. *J. Mater. Chem.* **2011**, *21*, 6999.